Organic & Biomolecular Chemistry

RSC Publishing

PAPER

View Article Online
View Journal | View Issue

Thiol-inducible direct fluorescence monitoring of drug release†

Cite this: *Org. Biomol. Chem.*, 2013, **11**, 580

Received 26th August 2012,
Accepted 2nd November 2012

DOI: 10.1039/c2ob26680f

www.rsc.org/obc

Jun Wu,‡[a] Rong Huang,‡[a] Changcheng Wang,[a] Wenting Liu,[a] Jiaqi Wang,[a] Xiaocheng Weng,[a] Tian Tian[a] and Xiang Zhou*[a,b]

A new bifunctional compound NCC, which undergoes thiol-mediated disulfide cleavage after cell entry, produces a red-shifted fluorescent emission in the cytosol and releases free active DNA alkylating agent CLB into the nucleus, and finally leads to DNA damage and cell death.

Introduction

Prodrugs are inactive compounds prior to administration. While upon exposure to specific physiological conditions, such as acidic, reducing and overexpressed enzymatic milieus, they are triggered to degrade or metabolize into an active therapeutic.[1–4] Novel chemotherapeutic drugs that can report on its localization and activation in cancer cells are being extensively investigated in the cancer treatment field.[5–8] Examples for selective tumor targeting include folate, cyclic peptides and galactose modified cytotoxic drugs (camptothecin and taxol) and prodrugs activated by hypoxia (tirapazamine).[9–15] However, it is difficult to establish precise delivery of a pharmaceutically activatable prodrug to cancer cells.[16,17] Toward this end, fluorescent probes that can provide a ready read-out under the typical conditions of cellular analysis are of particular interest. It would be desirable to develop a drug release system that contains both an active drug for efficacy and a fluorophore for monitoring.[18,19]

Results and discussion

Herein, we design a new compound naphthalimide–CLB conjugate (NCC) which is composed of a potent anticancer drug chlorambucil (CLB), a disulfide linker and a fluorescent naphthalimide moiety. NCC was prepared using a mature route with a satisfactory yield (Scheme 1), that is completely described in the Experiment section. CLB is an alkylating agent that is used to treat chronic lymphocytic leukemia through alkylation of the nuclear genome.[20–23] Additionally, the linkage disulfide bond is supposed to undergo cleavage *via* reaction with intracellular abundant thiols, such as glutathione or cysteine.[24–26] On the basis of disulfide cleavage, the fluorophore naphthalimide is released and leads to a distinctive ratiometric emission change. 4-Amino-1,8-naphthalimide is regarded as a useful fluorescent reporter group due to its unique ICT structure, large Stokes' shift, long emission wavelength and high quantum yield.[27–30] Our approach is illustrated in Scheme 2. As detailed below, NCC will become fluorescent activated in the cytosol upon cell entry that coincides with drug release into the nuclei, resulting in cell apoptosis.

Optical property studies

To demonstrate that the cleavage of the disulfide bond could be effected by treatment with thiols, DTT (1,4-dithiothreitol) was chosen to be used *in vitro* for the reaction with NCC, in consideration of its better liposolubility among commercially

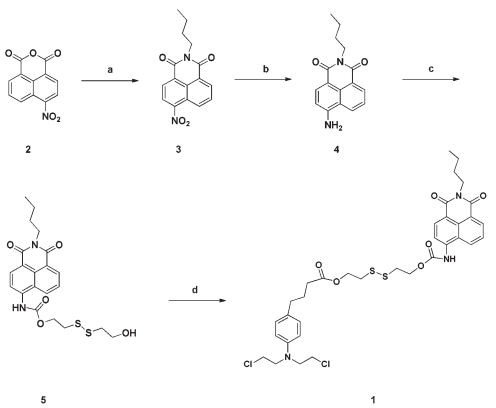

Scheme 1 Synthesis of NCC. (a) EtOH–butylamine; (b) Pd/C, H_2; (c) 2,2′-dithiodiethanol, tri-phosgene, DIPEA; (d) CLB, DCC, DMAP.

[a]*College of Chemistry and Molecular Sciences, Key Laboratory of Biomedical Polymers of Ministry of Education, State Key Laboratory of Virology, Wuhan University, Hubei, Wuhan, 430072, P. R. China. E-mail: xzhou@whu.edu.cn; Fax: +86-27-87336380; Tel: +86-27-61056559*

[b]*State Key Laboratory of Natural and Biomimetic Drugs, Beijing University, P. R. China*

†Electronic supplementary information (ESI) available. See DOI: 10.1039/c2ob26680f

‡These authors contributed equally to this work.

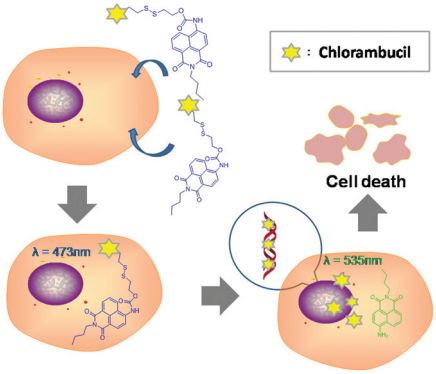

Scheme 2 Schematic representation of intracellular thiol mediated disulfide cleavage to induce fluorescent change and drug release.

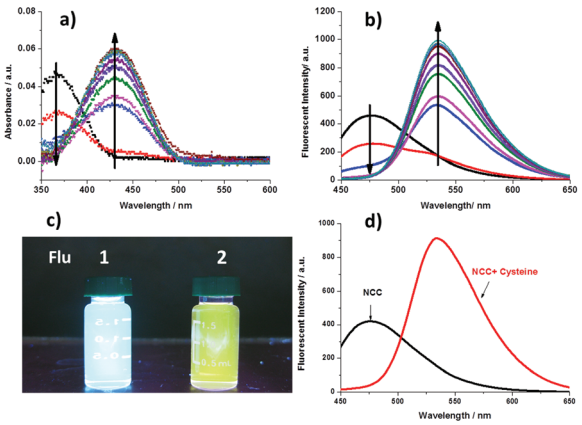

Fig. 1 (a) Absorption change and (b) fluorescence responses of NCC (10 μM) toward increasing concentrations of DTT (final concentration: 0, 0.01, 0.05, 0.1, 0.5, 1, 2, 4, 5, 6, 8, 10 mM) in sodium phosphate buffer (10 mM, pH = 7.5). Spectra were acquired 1 h after exposure to DTT at 37 °C. Excitation wavelength = 420 nm. (c) Fluorescence photographs of NCC in the absence (1) and presence (2) of DTT. (d) Fluorescence responses of NCC (10 μM) toward thiol-containing amino acid cysteine (5 mM) after 1 h incubation at 37 °C.

available thiols. The absorption and fluorescent spectra changes were monitored upon the addition of DTT under physiological conditions (phosphate buffer, pH 7.5, 37 °C). As shown in Fig. 1a and b, with the titration of DTT (0.01–10 mM), the broad absorption and emission peak centered in 370 and 475 nm, characteristic of NCC, gradually underwent a red-shift to 430 and 533 nm respectively, which corresponded to the product 4-aminonaphthalimide derivative. The ratio of fluorescence intensities (F_{533}/F_{475}) (λ_{ex} = 420 nm) changed from 0.4 to 35 (R = 87.5 fold). In this case, an easy-to-discern fluorescence change was visualized (Fig. 1c). The quantum yield of NCC (QY = 0.25) and naphthalimide derivative (QY = 0.10) were also determined by reference to known Quinine Sulfate. Similarly, we detected exactly the same fluorescent response of NCC toward cysteine, a thiol-containing amino acid which is essential in GSH. However, almost no appreciable fluorescent changes were observed upon exposure to nonthiol natural amino acids and biologically essential

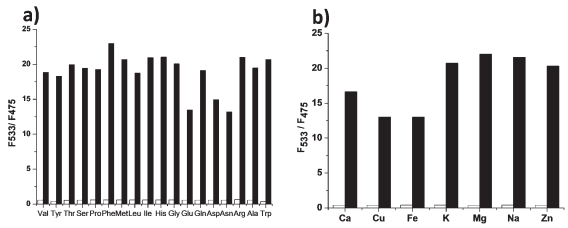

Fig. 2 (a) Fluorescence responses of NCC (10 μM) toward other nonthiol amino acids (5 mM respectively), including Val, Tyr, Thr, Ser, Pro, Phe, Met, Leu, Ile, His, Gly, Glu, Gln, Asp, Asn, Arg, Ala, Trp (white bars) and DTT (5 mM) in the presence of either nonthiol amino acid (black bars). (b) Fluorescence responses of NCC (10 μM) toward biologically relevant metal ions (Zn^{2+}, Na^{+}, Mg^{2+}, K^{+}, Fe^{3+}, Cu^{2+} and Ca^{2+}, 1 mM respectively). Bars represent fluorescence intensity ratio F_{533}/F_{475}. Each spectrum was acquired 1 h after exposure to the analytes at 37 °C. Excitation wavelength = 420 nm.

metal ions (Fig. 2a and b). Moreover, the effects of the above-mentioned thiol-free analytes and metal ions on DTT inducing cleavage were excluded, as the results show that NCC possesses high selectivity toward DTT when present with these interferents simultaneously.

Efforts were made to investigate the time-dependent fluorescent variation. In Fig. S1,† the emission intensity at 475 nm was seen to increase initially in the first two minutes, then decrease gradually. Meanwhile, the emission at 533 nm was markedly enhanced within 15 min, and then reached a plateau. Furthermore, the pH dependence of the DTT-induced emission change was assessed (Fig. S2†). It shows that NCC provides a stable low background signal within a pH range of 2–10. On the other hand, its response ability toward DTT is invariable within the biologically relevant pH range (7–9). Therefore, NCC can readily react with the cellular thiols without pH effects.

Proposed mechanism of thiol-inducing cleavage

The mechanisms by which the thiol-inducing reaction are postulated to occur are illustrated in Scheme 3. Complementary HPLC analysis of the DTT-treated NCC solution demonstrated the generation of the final fluorescent product naphthalimide.

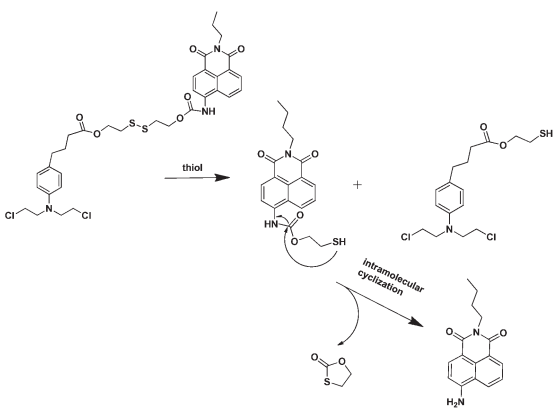

Scheme 3 Proposed mechanism corresponding to the reaction of NCC with thiol.

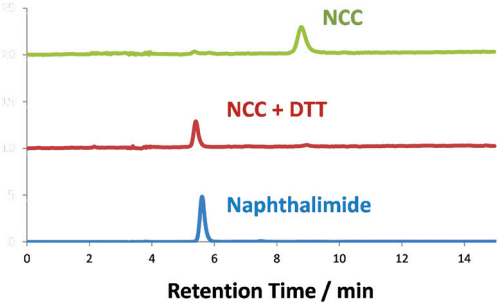

Fig. 3 The HPLC analysis of NCC without treatment of DTT (top); with DTT treatment for 2 h at 37 °C (middle); fluorescent naphthalimide only (bottom). The retention time at 8.9 min corresponds to NCC while the retention time at 5.6 min corresponds to fluorescent product naphthalimide. The signals were monitored at 503 nm under the irradiation at 382 nm.

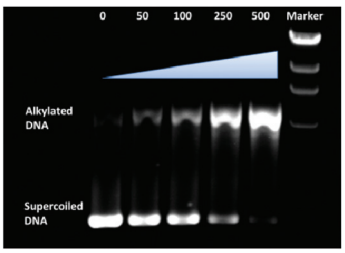

Fig. 4 Agarose gel of plasmid DNA (pBR322) incubated at 37 °C for 12 h with NCC in the presence of 10 mM GSH. The concentrations of NCC are 50, 100, 250, 500 μM respectively. The first lane is control DNA and the last lane is DNA marker.

As shown in Fig. 3, the peak at the retention time of 8.9 min, which corresponded to NCC, disappeared after incubation with DTT. Instead, a new peak with an identical retention time to naphthalimide (t = 5.6 min) was observed. All these results confirm that DTT triggers the disulfide cleavage of NCC and produces a unstable thiol intermediate, which consequently undergoes a rapid intramolecular cyclization to releases naphthalimide for fluorescent signal activation.

DNA alkylation *in vitro*

As CLB is a DNA alkylating agent, the DNA interacting ability of NCC upon exposure to GSH was evaluated by denatured alkaline agarose gel electrophoresis (Fig. 4). After incubation for 12 h with 10 mM GSH at 37 °C, NCC produced nearly 100% DNA alkylation at a concentration of 500 μM. The non-reacted supercoiled plasmid DNA (pBR322), which was present in lower bands, exhibited a dose-dependent decrease in accordance with the formation of alkylated DNA in higher bands. Hence, NCC is confirmed to trigger DNA damage *in vitro*. Meanwhile, the well-studied alkylating mechanism of CLB is presented in Scheme S1.† The lone pair developed on CLB can form a highly electrophilic intermediate aziridinium ring by intramolecular displacement of the chloride by the amine nitrogen. This electrophilic intermediate greatly facilitates the DNA alkylation and cross-linking formation.

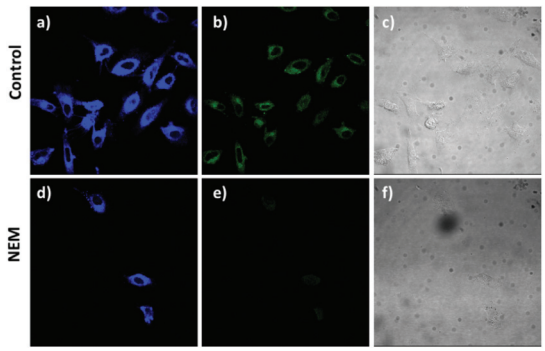

Fig. 5 Confocal fluorescence images of thiol-blocking experiment. HeLa cells incubated with NCC (10 μM) for 1 h (a–c), HeLa cells incubated with NCC (10 μM) for 1 h after pretreatment with 2.5 mM NEM for 12 h (d–f). (a, d) blue channel at 450 ± 35 nm, (b, e) green channel at 515 ± 30 nm, (c, f) bright-field image. Incubation was performed at 37 °C under a humidified atmosphere containing 5% CO_2. Wavelength of excitation laser is 405 nm.

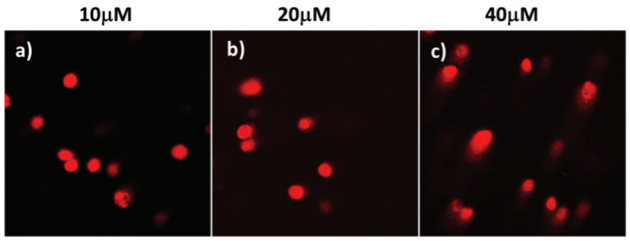

Fig. 6 Alkaline comet assay for HeLa cells treated with NCC (10, 20 and 40 μM) for 48 h. Nuclear DNA was stained by PI (propidium iodide, a red fluorescent dye).

Intracellular imaging

To determine the fluorescence change of NCC in living cells, confocal microscopy was performed. HeLa cells incubated with 10 μM NCC for 1 h displayed intense intracellular fluorescence at both blue and green channels (Fig. 5a–c). Further to confirm such emission resulted from the disulfide cleavage reaction, a thiol-blocking experiment was conducted. HeLa cells were pretreated with 2.5 mM NEM (*N*-ethylmaleimide) for 12 h to downregulate biological thiols and then incubated with NCC for another 1 h. As expected, the fluorescence intensity at the green channel significantly decreased (Fig. 5d–f). All the results suggest that thiol-induced disulfide cleavage of NCC occurs in the cytosol and releases the drug CLB simultaneously, which presumably diffuses into the nucleus to function as DNA alkylating agent.

DNA alkylation in cell systems

The anticancer activity of NCC was evaluated by MTT assay (Fig. S3†). When HeLa cells were treated with NCC (10 nM–500 μM) for 72 h, a distinct dose-dependent decrease in cell viability was observed with a IC_{50} value of 28.8 ± 0.8 μM. To explain the origin of cytotoxicity, an alkaline comet assay related to DNA damage was visually performed and is shown in Fig. 6. Stained by nuclear red dye PI, the extent of cellular DNA damage increased with increasing concentration of NCC

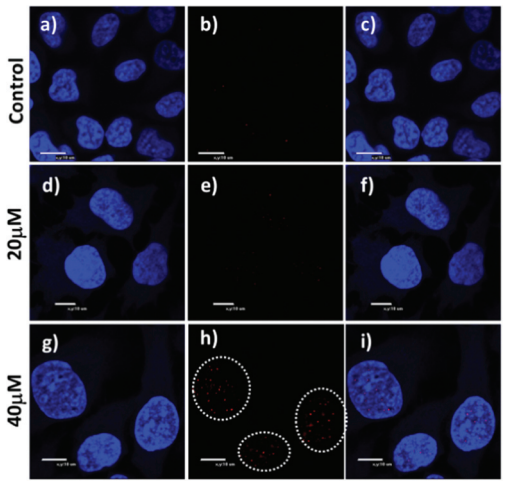

Fig. 7 γ-H2AX immunofluorescence in HeLa cells after incubation without and with 20, 40 μM NCC for 48 h. The white dotted circles indicate γ-H2AX foci (red) and the Hoechst 33 258 dye (blue) localizes the nuclear DNA. Images (a, d, g) were obtained from blue channel at 450 ± 35 nm with excitation wavelengths of 405 nm, images (b, e, h) were obtained from red channel at 605 ± 35 nm with excitation wavelengths of 543 nm, and images (c, f, i) are merged photographs of the two channels. Scale bar, 10 μm.

(10–40 μM), resulting in random DNA strand breaks and short DNA fragment migrations which are observed as comet tails. At a dose of 40 μM, NCC displayed an obvious comet image, indicating that it reached target DNA inside the cell and produced DNA damage as well.

As DNA interstrand cross-links can completely block replication and transcription and may also generate double stand breaks (DSBs) during its repair, γ-H2AX immuno-fluorescence microscopy is a well-accepted and sensitive method to detect DSBs. After exposure of cells to DSB-inducing agents, the histone protein H2AX is rapidly phosphorylated on Ser139 as a signal of DNA damage response.[31,32] In Fig. 7, it is noteworthy that 40 μM NCC triggered prominent red γ-H2AX foci in the HeLa cell nucleus. In contrast, the control cells did not show noticeable DNA damage. Therefore, these results confirm that the thiol-activated cross-linking of NCC induces cytotoxic DNA damage.

Conclusion

In summary, we have developed a multicomponent synthetic strategy which allows for fluorescence-activatable monitoring of the release of an anticancer drug. NCC takes advantage of biologically abundant thiols to trigger disulfide bond cleavage, with subsequent release of naphthalimide moiety as a ratiometric fluorescent reporter and CLB as a DNA alkylating agent to induce DNA damage. This approach can provide both therapeutic effect evaluation and drug delivery imaging information, ensuring improved understanding of cellular uptake and release mechanisms of drugs. Additional exploration and modification of the compound NCC could lead to the ability to release drugs specifically at the diseased site in a more intuitive and controllable manner.

Experimental section

Synthesis of compound 3

To a mixture of compound **2** (486.4 mg, 2 mmol) in 50 mL EtOH was added butylamine (204.8 mg, 2.8 mmol), the resulting solution was stirred at reflux temperature for 12 h. After cooling to room temperature, the solvent and excess butylamine were removed under reduced pressure and the residue was subjected to flash column chromatography with ethyl acetate–cyclohexane (1 : 12, v/v) as eluent to give the desired product as a light yellow solid (416 mg, 70%). ^{1}H NMR (300 MHz, $CDCl_3$): δ 8.76 (d, J = 8.1 Hz, 1 H), 8.67–8.60 (m, 2 H), 8.29 (d, J = 7.8 Hz, 1 H), 7.91 (t, J = 7.8 Hz, 1 H), 4.12 (t, J = 6.9 Hz, 2 H), 1.65–1.62 (m, 2 H), 1.39–1.37 (m, 2 H), 0.91 (t, J = 6.9 Hz, 3 H); ^{13}C NMR (300 MHz, $CDCl_3$): δ 163.5, 162.7, 149.7, 132.6, 130.2, 129.9, 129.4, 127.3, 124.1, 123.3, 40.8, 30.3, 20.5, 14.0 ppm; ESI-MS found m/z = 298.3 $[M]^+$.

Synthesis of compound 4

This compound was synthesized by hydrogenating **3** (400 mg, 1.34 mmol) in MeOH–$CHCl_3$ (1 : 1) at 30 °C under hydrogen atmosphere in the presence of 10% Pd/C catalyst for 24 h. The reaction mixture was filtered, and washed with MeOH and $CHCl_3$. The filtrate was evaporated under reduced pressure to yield the product as a orange solid (346.6 mg, 95%). ^{1}H NMR (300 MHz, $CDCl_3$): δ 8.58 (d, J = 7.8 Hz, 1 H), 8.40 (d, J = 6.0 Hz, 1 H), 8.09 (d, J = 8.1 Hz, 1 H), 7.64 (t, J = 6.0 Hz, 1 H), 6.88 (d, J = 7.5 Hz, 1 H), 4.93 (s, 2 H), 4.14 (t, J = 5.7 Hz, 3 H), 1.71–1.68 (m, 2 H), 1.44–1.41 (m, 2 H), 0.95 (t, J = 5.7 Hz, 3 H); ^{13}C NMR (300 MHz, $CDCl_3$): δ 164.4, 163.5, 153.4, 134.6, 131.6, 130.3, 130.0, 124.6, 122.4, 120.0, 108.8, 108.2, 39.7, 30.5, 20.5, 14.4; ESI-MS found m/z = 267.7 $[M - H]^-$.

Synthesis of compound 5

To a mixture of **4** (0.2 g, 0.74 mmol) and tri-phosgene (0.4 g, 1.4 mmol) in 50 mL of dichloromethane was added DIPEA (0.5 mL, 2.5 mmol) dropwise at 0 °C. The resulting solution was stirred for 1 h at room temperature. And then 2,2′-dithiodiethanol (0.6 g, 3.5 mmol) in CH_2Cl_2 (5 mL) was added to the solution and the reaction mixture was stirred for 24 h at room temperature. The solvent was evaporated off, at which point $CHCl_3$ (100 mL) and water (100 mL) were added, and the organic layer was collected. The $CHCl_3$ layer was dried over anhydrous $NaSO_4$. After removal of the solvents, the crude product was purified over silica gel using ethyl acetate–hexanes (v/v, 1 : 3) as the eluent to yield **5** as a yellow solid (169 mg, 51%). ^{1}H NMR (300 MHz, $CDCl_3$): 8.59 (m, 2 H), 8.34 (d, 1 H, J = 8.2 Hz), 8.22 (d, 1 H, J = 8.5 Hz), 7.73 (br, 1 H), 7.27 (t, 1 H, J = 8.0 Hz), 4.56 (t, 2 H, J = 6.3 Hz), 4.14 (d, 2 H, J = 7.5 Hz), 3.94 (t, 2 H, J = 5.6 Hz), 3.07 (t, 2 H, J = 6.3 Hz), 2.96 (t, 2 H, J = 5.8 Hz), 2.24 (br, 1 H), 1.69–1.60 (m, 2 H), 1.58–1.43 (m, 2 H), 0.97 (t, 3 H, J = 7.3 Hz). ^{13}C NMR ($CDCl_3$, 300 MHz):

164.1, 163.6, 152.9, 138.8, 132.4, 131.2, 128.8, 126.6, 126.1, 123.3, 123.0, 117.9, 116.9, 63.8, 60.5, 41.5, 40.2, 37.4, 30.2, 20.4, 13.8 ppm. ESI-MS found 449.1 [M + H^+].

Synthesis of compound 1 (NCC)

N,*N*′-Dicyclohexylcarbodiimide (DCC: 50 mg, 0.24 mmol) was added to a stirred solution of **5** (100 mg, 0.22 mmol), chlorambucil (CLB: 67 mg, 0.22 mmol), and 4-dimethyl-aminopyridine (DMAP: 5 mg, 0.02 mmol) in CH_2Cl_2 (5 mL) at 0 °C. The solution was stirred for 24 h at room temperature. After removal of dicyclohexylurea by filtration, the filtrate was successively washed with water (3 × 10 mL) and a saturated solution of NaCl (5 mL). The solution was dried over $NaSO_4$ and the solvent removed *in vacuo*. The crude product was purified over silica gel using ethyl acetate–hexanes (v/v, 1 : 10) as the eluent to yield **5** as a yellow solid (67 mg, 42%). ^{1}H NMR (300 MHz, $CDCl_3$): 8.61 (m, 2H), 8.35 (d, 1H, J = 8.2 Hz), 7.96 (d, 1H, J = 8.5 Hz), 7.70–6.98 (m, 2H), 6.60–6.57 (m, 2H), 4.54 (t, 2H, J = 6.3 Hz), 4.41 (d, 2H, J = 7.5 Hz), 4.17 (t, 2H, J = 6.3 Hz), 4.02 (d, 2H, J = 7.5 Hz), 3.67 (d, 4H, J = 5.6 Hz), 3.61 (d, 4H, J = 5.6 Hz), 3.04 (t, 2H, J = 6.3 Hz), 2.96 (t, 2H, J = 5.8 Hz), 2.46 (br, 1H), 1.87 (d, 2H, J = 7.5 Hz), 1.43 (m, 2H), 1.25 (m, 2H), 0.97 (t, 3H, J = 7.3 Hz). ^{13}C NMR ($CDCl_3$, 300 MHz): 173.7, 163.6, 153.0, 144.3, 132.3, 131.1, 129.5, 126.4, 123.3, 117.0, 112.1, 67.29, 62.9, 62.4, 53.5, 40.4, 40.1, 37.6, 36.5, 33.8, 33.5, 32.2, 30.1, 26.6, 20.3, 18.6, 13.7, 13.5 ppm. HRMS (ESI): *m*/*z*: calcd for $C_{35}H_{41}Cl_2N_3O_6S_2$ + Na: 756.1712; found: 756.1710 [M^+ + Na]; melting range: 175–177 °C.

Optical properties study

Fluorescent emission spectra were collected from 460–650 nm on PerkinElmer LS 55 with an excitation wavelength of 380 nm, the excitation and emission slit widths were 15 and 9 nm. Quartz cuvettes with 2 mL volume used for emission measurements. UV-Vis absorption spectra were collected on a SHIMADZU UV-2550 from 350–600 nm with 600 μL quartz cuvettes. Unless otherwise specified, all spectra were taken at 37 °C in 10 mM sodium phosphate buffers.

For determination of the quantum efficiency of fluorescence (Y_u), quinine sulfate in water (Y_s = 0.54) was used as a standard. Values were calculated according to the following equation.

$$Y_u = Y_s \times \frac{F_u}{F_s} \times \frac{A_s}{A_u}$$

where s means standard, u means sample, A means absorbance at the excitation wavelength, F means integrated area under the fluorescence spectra on an energy scale.

Cell culture

HeLa human cervical carcinoma cells (CCTCC, China) were cultured in MEM (Hyclone, China) supplemented with 10% FBS, penicillin (100 units per mL), and streptomycin (100 μg mL^{-1}). All the cells were maintained in a humidified atmosphere of 5/95 (v/v) of CO_2–air at 37 °C.

Cell survival assay

Cells were harvested using trypsin and washed with PBS. The cells were added into a 96-well plate with 5000 cells per well and incubated overnight for attachment at 37 °C in a 5% CO_2 incubator. The following day, cells were treated with the compounds (10 nM–500 μM) for 72 h. Control cells (without any compound) were treated under the exact same conditions. After the incubation period, cell survival was evaluated using an MTT assay: 10 μL of a freshly prepared solution of MTT (5 mg mL^{-1} in PBS) was added to each well, and after 4 h incubation, the medium was removed; upon addition of 100 μL of DMSO to each well, the optical density values were detected at 492 nm. Cytotoxicity data were expressed as IC_{50} values. Data were expressed as mean values of three individual experiments conducted in triplicate.

Confocal imaging of thiol-blocking experiment

10^5 Cells seeded on two 35 mm glass-bottomed dishes (Nest) were washed with 1 mL PBS. One dish of cells was incubated with NADH-CLB (10 μM) for 1 h; the other dish of cells was incubated with NADH-CLB (10 μM) for 1 h after pretreatment with 2.5 mM NEM for 12 h, and then both of them were mounted on the microscope stage. The light source was a white-light laser. The excitation wavelength was 405 nm. Blue channel at 450 ± 35 nm and green channel at 515 ± 30 nm.

Alkaline comet assay

Cells were plated (4 × 10^4 cells per well) onto six-well plates to a final volume of 2 mL and allowed an overnight period for attachment. Next, each dilution of t NADH-CLB (10–40 μM) was added per well, and the mixtures were incubated at 37 °C for 48 h. After 48 h of incubation, the medium was removed and replaced with HBSS solution, after which the cells were scraped off. A total of 100 μL of cells was suspended in 700 μL of 1% low-melting-point agarose and precoated with 1% normal-melting-point agarose. Cells were lysed overnight at 4 °C in cold alkaline lysis buffer (1% fresh Triton X-100, 2.5 M NaCl, 100 mM EDTA, and 10 mM Tris-HCl, pH 10.0). The agarose gels were immersed into alkaline electrophoresis buffer (300 mM NaOH and 1 mM EDTA at pH > 13) for 30 min, and then subjected to electrophoresis in the same buffer at 25 V and 300 mA for 40 min. The gels were then rinsed with neutralization buffer (0.4 M Tris-HCl, pH 7.5) three times and left to air-dry, after which they were stained with 10 μg mL^{-1} propidium iodide and incubated for 20 min. Finally, images were analyzed using a Nikon confocal laser scanning microscope.

γ-H2AX Immunofluorescence assay

Cells plated on a 35 mm glass-bottomed culture dish were fixed for 20 min and then washed in 0.5% Triton X-100/PBS. The cells were then treated with permeabilization buffer [20 mmol L^{-1} Tris-HCl (pH 8), 0.5% Triton X-100, 50 mmol L^{-1} NaCl, 3 mmol L^{-1} $MgCl_2$, and 300 mmol L^{-1} sucrose] for 15 min at 37 °C, washed twice with PBS, and then stained with

1 μg mL^{-1} γ-H2AX (phosphor S139) rabbit polyclonal antibody at 4 °C overnight. Secondary antibodies raised against rabbit with red fluorescent tetramethylrhodamine isothiocyanate were incorporated and the nuclear DNA was stained with 5 μg L^{-1} Hoechst 33258, after which images were analyzed using a Nikon confocal laser scanning microscope.

Acknowledgements

The authors thank the National Basic Research Program of China (973Program) (2012CB720600, 2012CB720603, 2012CB 720605), the National Science of Foundation of China (No. 91213302, 30973605, 21072115), the National Grand Program on Key Infectious Disease (2012ZX10003002-014). Supported by Program for Changjiang Scholars and Innovative Research Team in University (IRT1030).

Notes and references

1 M. C. Parrott, M. Finniss, J. C. Luft, A. Pandya, A. Gullapalli, M. E. Napier and J. M. DeSimone, *J. Am. Chem. Soc.*, 2012, **134**, 7978–7982.
2 K. M. Huttunen, H. Raunio and J. Rautio, *Pharmacol. Rev.*, 2011, **63**, 750–771.
3 L. Bildstein, C. Dubernet and P. Couvreur, *Adv. Drug Delivery Rev.*, 2011, **63**, 3–23.
4 J. Rautio, H. Kumpulainen, T. Heimbach, R. Oliyai, D. Oh, T. Järvinen and J. Savolainen, *Nat. Rev. Drug Discovery*, 2008, **7**, 255–270.
5 P. S. Low, W. A. Henne and D. D. Doorneweerd, *Acc. Chem. Res.*, 2008, **41**, 120–129.
6 S. Santra, C. Kaittanis, O. J. Santiesteban and J. M. Perez, *J. Am. Chem. Soc.*, 2011, **133**, 16680–16688.
7 K. Kim, M. Lee, H. Park, J. H. Kim, S. Kim, H. Chung, K. Choi, I. S. Kim, B. L. Seong and I. C. Kwon, *J. Am. Chem. Soc.*, 2006, **128**, 3490–3491.
8 F. Wang, Y. C. Wang, S. Dou, M. H. Xiong, T. M. Sun and J. Wang, *ACS Nano*, 2011, **5**, 3679–3692.
9 J. W. Lee, J. Y. Lu, P. S. Low and P. L. Fuchs, *Bioorg. Med. Chem.*, 2002, **10**, 2397–2414.
10 W. A. Henne, D. D. Doorneweerd, A. R. Hilgenbrink, S. A. Kularatne and P. S. Low, *Bioorg. Med. Chem. Lett.*, 2006, **16**, 5350–5355.
11 M. H. Lee, J. H. Han, P. S. Kwon, S. Bhuniya, J. Y. Kim, J. L. Sessler, C. Kang and J. S. Kim, *J. Am. Chem. Soc.*, 2012, **134**, 1316–1322.
12 M. H. Lee, J. Y. Kim, J. H. Han, S. Bhuniya, J. L. Sessler, C. Kang and J. S. Kim, *J. Am. Chem. Soc.*, 2012, **134**, 12688–12674.
13 J. M. Brown, *Cancer Res.*, 1999, **59**, 5863–5870.
14 J. M. Brown and W. R. Wilson, *Nat. Rev. Cancer*, 2004, **4**, 437–447.
15 V. Junnotula, U. Sarkar, S. Sinha and K. S. Gates, *J. Am. Chem. Soc.*, 2009, **130**, 1015–1024.
16 C. P. Leamon, J. A. Reddy, I. R. Vlahov, M. Vetzel, N. Parker, J. S. Nicoson, L. C. Xu and E. Westrick, *Bioconjugate Chem.*, 2005, **16**, 803–811.
17 C. P. Leamon, I. Pastan and P. S. Low, *J. Biol. Chem.*, 1993, **268**, 24847–24854.
18 R. Weinstain, E. Segal, R. Satchi-Fainaro and D. Shabat, *Chem. Commun.*, 2010, **46**, 553–555.
19 D. W. Domaille, E. L. Que and C. J. Chang, *Nat. Chem. Biol.*, 2008, **4**, 168–175.
20 S. B. Fonseca, M. P. Pereira, R. Mourtada, M. Gronda, K. L. Horton, R. Hurren, M. D. Minden, A. D. Schimmer and S. O. Kelley, *Chem. Biol.*, 2011, **18**, 445–453.
21 J. Hebb, S. Assouline, C. Rousseau, P. Desjardins, S. Caplan, M. J. Egorin, L. Amrein, R. Aloyz and L. Panasci, *Cancer Chemother. Pharmacol.*, 2011, **68**, 643–651.
22 A. Begleiter, M. Mowat, L. G. Israels and J. B. Johnston, *Leuk. Lymphoma*, 1996, **23**, 187–201.
23 C. M. Clavel, O. Zava, F. Schmitt, B. H. Kenzaoui, A. A. Nazarov, L. Juillerat-Jeanneret and P. J. Dyson, *Angew. Chem., Int. Ed.*, 2011, **50**, 7124–7127.
24 X. Guo, X. Qian and L. Jia, *J. Am. Chem. Soc.*, 2004, **126**, 2272–2273.
25 T. T. Beaudette, J. A. Cohen, E. M. Bachelder, K. E. Broaders, J. L. Cohen, E. G. Engleman and J. M. Frechet, *J. Am. Chem. Soc.*, 2009, **131**, 10360–10361.
26 C. P. Leamon, J. A. Reddy, I. R. Vlahov, M. Vetzel, N. Parker, J. S. Nicoson, L. C. Xu and E. Westrick, *Bioconjugate Chem.*, 2005, **16**, 803–811.
27 B. Zhu, X. Zhang, Y. Li, P. Wang, H. Zhang and X. Zhuang, *Chem. Commun.*, 2010, **46**, 5710–5712.
28 H. He, M. A. Mortellaro, M. J. Leiner, R. J. Fraatz and J. K. Tusa, *J. Am. Chem. Soc.*, 2003, **125**, 1468–1469.
29 H. He, M. A. Mortellaro, M. J. Leiner, S. T. Young, R. J. Fraatz and J. K. Tusa, *Anal. Chem.*, 2003, **75**, 549–555.
30 J. F. Zhang, C. S. Lim, S. Bhuniya, B. R. Cho and J. S. Kim, *Org. Lett.*, 2011, **13**, 1190–1193.
31 M. Bai, J. Huang, X. Zheng, Z. Song, M. Tang, W. Mao, L. Yuan, J. Wu, X. Weng and X. Zhou, *J. Am. Chem. Soc.*, 2010, **132**, 15321–15327.
32 R. Rodriguez, K. M. Miller, J. V. Forment, C. R. Bradshaw, M. Nikan, S. Britton, T. Oelschlaegel, B. Xhemalce, S. Balasubramanian and S. P. Jackson, *Nat. Chem. Biol.*, 2012, **8**, 301–310.